Bioinspired programmable wettability arrays for droplets manipulation

Lingyu Sun[a,b], Feika Bian[b], Yu Wang[b], Yuetong Wang[b], Xiaoxuan Zhang[b], and Yuanjin Zhao[a,b,1]

[a]Department of Clinical Laboratory, The Affiliated Drum Tower Hospital of Nanjing University Medical School, 210008 Nanjing, China; and [b]State Key Laboratory of Bioelectronics, School of Biological Science and Medical Engineering, Southeast University, 210096 Nanjing, China

Edited by David A. Weitz, Harvard University, Cambridge, MA, and approved January 22, 2020 (received for review December 4, 2019)

The manipulation of liquid droplets demonstrates great importance in various areas from laboratory research to our daily life. Here, inspired by the unique microstructure of plant stomata, we present a surface with programmable wettability arrays for droplets manipulation. The substrate film of this surface is constructed by using a coaxial capillary microfluidics to emulsify and pack graphene oxide (GO) hybrid *N*-isopropylacrylamide (NIPAM) hydrogel solution into silica nanoparticles-dispersed ethoxylated trimethylolpropane triacrylate (ETPTA) phase. Because of the distribution of the silica nanoparticles on the ETPTA interface, the outer surface of the film could achieve favorable hydrophobic property under selective fluorosilane decoration. Owing to the outstanding photothermal energy transformation property of the GO, the encapsulated hydrophilic hydrogel arrays could shrink back into the holes to expose their hydrophobic surface with near-infrared (NIR) irradiation; this imparts the composite film with remotely switchable surface droplet adhesion status. Based on this phenomenon, we have demonstrated controllable droplet sliding on programmable wettability pathways, together with effective droplet transfer for printing with mask integration, which remains difficult to realize by existing techniques.

bioinspired | wettability | droplet | microfluidics | printing

Controllable manipulation on small quantities of fluids has aroused enormous interest and research for its broad application prospects in chemical reaction, medical diagnosis, biological analysis, and so on (1–7). Up to date, various methods have been developed for maneuvering the droplets under various external forces, including electric (8, 9), acoustic wave (10, 11), magnetism (12, 13), light (14), and wettability gradients (15). Among them, techniques based on wettability surfaces for droplet manipulation are an ideal choice because of their unparalleled advantages in simplification and efficiency (16–21). In particular, surfaces with tunable wettability are capable of manipulating the pinning and sliding of droplets in a reversible manner responding to external stimulation, showing superiority of intelligence and controllability (22–24). Based on these virtues, the tunable wettability surfaces have demonstrated potential value in various fields, such as fog collection (25), droplet transportation (26), cell adhesion (27, 28), etc. Although with many successes, most of the existing wettability surfaces could only exhibit uniform wettability control behavior and thus were difficult to accurately manipulate droplets to a certain location or multiple locations, these demands are usually necessary for the droplets' manipulation in practical applications. Therefore, functional surfaces with programmable wettability locations are still anticipated to extend their practical values in droplets manipulation.

In this paper, inspired by the microstructure of stomata distributed on plants, we proposed programmable wettability arrays for droplets manipulation by using microfluidic emulsification templates, as shown in Fig. 1. Stomata are unique construction of plants surrounded by a pair of guard cells with a hydraulic gating function, which can automatically convert the opening and closing status to regulate the gas exchange with environment. By integrating the stomata structurelike stimuli-responsive property into membranes, bionicists have created many intelligent materials involving smart valves, biosensors, and so on (29, 30). Microfluidics is a platform with integrated channels on the microscale for precisely controlling and manipulating small quantities of fluids. Because of its profound scientific and engineering standards, microfluidics has been considered as an outstanding and versatile technology for fabricating template materials with controllable morphology and functions (31–37), although with many successes, both of the plant stomata inspiration and microfluidic techniques have not been employed for constructing wettability arrays with these integrated advantages.

Here, we fabricated the desired surfaces with wettability arrays by using a coaxially assembled capillary microfluidic device to emulsify graphene oxide (GO) hybrid *N*-isopropylacrylamide (NIPAM) hydrogel solution into silica nanoparticles-dispersed ethoxylated trimethylolpropane triacrylate (ETPTA) phase. Through tuning the proportion of the two phases and polymerizing them, films with interconnected hydrogel microsphere array structured surfaces could be obtained. As the silica nanoparticles were distributed on the ETPTA interface, the outer surface of the films could gain favorable hydrophobic property under fluorosilane evaporation, without affecting the hydrophilic hydrogel arrays. Benefitting from the excellent photothermal energy transformation feature of the GO (38, 39), the encapsulated hydrogel microsphere arrays were imparted with near-infrared (NIR)-responsive capability. During the process, the hydrophilic hydrogel arrays would shrink back into interconnected holes to expose the hydrophobic surface; this made the composite system switch its surface droplet adhesion status under remote NIR

Significance

Droplet manipulation has received great attention and research for its potential applications in various fields. Wettability surfaces, especially tunable wettability surfaces, are efficient way to manipulate the pinning and sliding of droplets. However, these surfaces only demonstrate uniform wettability control behavior and thus were difficult to accurately manipulate droplets to a certain location or multiple locations. In this paper, inspired by the microstructure of stomata distributed on plants, we present programmable wettability arrays for droplets manipulation by using microfluidic emulsification templates. Based on the intelligent composite system, controllable droplet sliding on programmable wettability pathways and effective droplet transfer for printing with mask integration have been demonstrated.

Author contributions: Y.Z. designed research; L.S. performed research; L.S., F.B., Yu Wang, Yuetong Wang, and X.Z. analyzed data; and L.S. and Y.Z. wrote the paper.

The authors declare no competing interest.

This article is a PNAS Direct Submission.

[1]To whom correspondence may be addressed. Email: yjzhao@seu.edu.cn.

This article contains supporting information online at https://www.pnas.org/lookup/suppl/doi:10.1073/pnas.1921281117/-/DCSupplemental.

First published February 18, 2020.

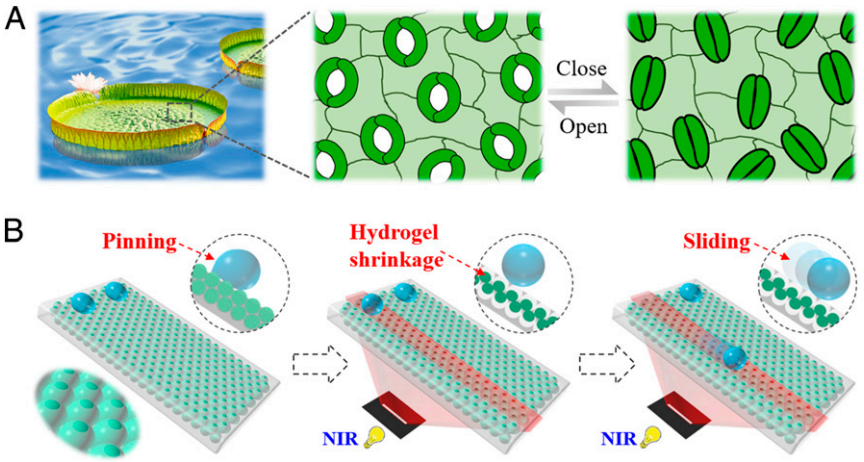

Fig. 1. (*A*) The stomata distributed on plants would open or close according to the environment. (*B*) Similar to the stimuli-responsive capacity of stomata, the functional surface could also switch its water adhesion capacity for controllable droplet sliding on programmable wettability pathway under remote NIR irradiation.

irradiation. With this feature, controllable droplet sliding on programmable wettability pathways, as well as effective droplet transfer for printing by integrating mask without preprogramming, have also been demonstrated. These results indicate that the bioinspired surfaces with programmable wettability arrays are valuable for different applications.

Results

In a typical experiment, the surfaces with wettability arrays were fabricated by single microfluidic emulsion templates, as shown in Fig. 2*A*. The microfluidic device for emulsification was coaxially assembled by inner and outer capillaries. In this system, GO hybrid NIPAM solution was utilized as dispersed phase while silica nanoparticles-dispersed ETPTA was employed as continuous phase, respectively. When these fluids were pumped into the device, highly uniform GO-NIPAM droplets were generated at the end of the inner capillary (*SI Appendix*, Fig. S1). The generated droplets were collected by a container filled with silica nanoparticles-dispersed ETPTA solution and spontaneously formed close-packed hexagonal structure at the air–water interface to minimize the free energy of the whole system (Fig. 2*C*). After being polymerized by UV light and washed by ethanol, films with interconnected hydrogel microsphere array structured surfaces were obtained, as shown in Fig. 2*D*. During the process, the droplet size could be adjusted by the flow-rate ratio of these two phases (Fig. 2*B*). The relationship between droplet size and flow rate, as well as the uniformity of droplets were explored and recorded to demonstrate the controllability of microfluidic technique (*SI Appendix*, Fig. S1). To investigate the microstructure of resultant films, a scanning electron microscope (SEM) was employed to observe and record the results after vacuum freeze drying. It was demonstrated that the hydrogel arrays showed dense packing arrangement in the film (Fig. 2*E*) and porous structure (Fig. 2*G*) after freeze-drying treatment. Additionally, silica nanoparticles were distributed on the ETPTA

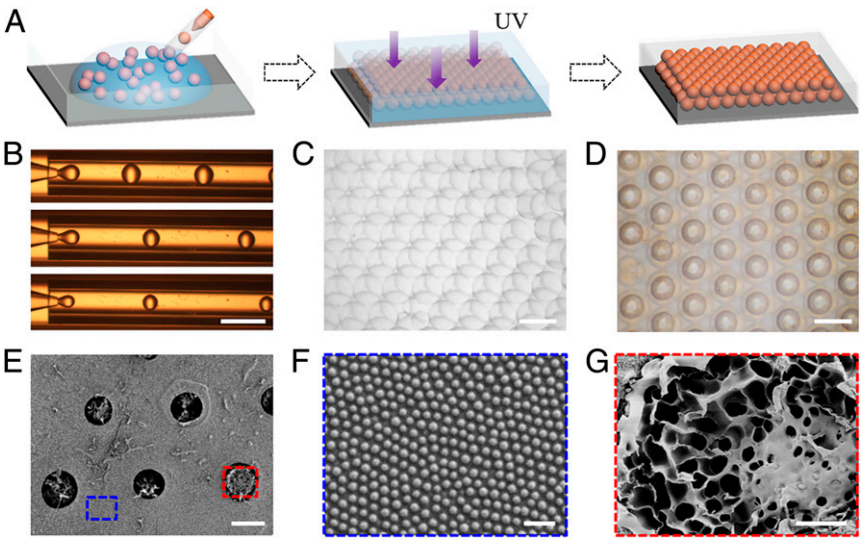

Fig. 2. (*A*) Scheme of the fabrication process of surfaces with wettability arrays by using microfluidic templates. (*B*) The generation process of microfluidic emulsification templates. (*C*) Optical image of the self-assembled GO-NIPAM droplets. (*D*) Optical image of the polymerized surface with wettability arrays. (*E*) SEM image of the functional surface. (*F*) Silica nanoparticles distributed on the ETPTA surface. (*G*) The porous microstructure of composite hydrogel. (Scale bar: 1 cm, 250 μm, 250 μm, 100 μm, 1 μm, and 20 μm in *B*–*G*, respectively.)

interface (Fig. 2*F*), facilitating the following hydrophobic treatment because of their abundant groups.

In general, the hydrophobic property results from the combined action of the chemical composition and micro- or nanostructure of the material surface. Therefore, to obtain hydrophobic property, the fabricated porous surfaces were further decorated by a low surface energy layer (perfluorodecyl trimethoxysilane). As a result, the water contact angle (2 μL) could reach 145°, much superior to the value (100°) before treatment (*SI Appendix*, Fig. S2). Besides, because of the photothermal effect of GO, the wettability hydrogel arrays were imparted with programmable capability under NIR control. To verify the existence of GO, a Raman spectrum was conducted to measure the characteristic peaks (*SI Appendix*, Fig. S3). The result showed that the typical D and G band peaks appeared at 1,360 cm^{-1} and 1,590 cm^{-1}, respectively, and the ID/IG ratio was 0.94, corresponding to the recognized value of GO. When the resultant surface was exposed to NIR, GO could transfer the optical energy into heat energy with high efficiency. Once the temperature increased to lower critical solution temperature of NIPAM, the hydrogel would shrink back to holes in seconds. The shrinkage of hydrophilic hydrogel led to the exposing of hydrophobic ETPTA substrate, thus switching the water adhesion capacity of the composite system (*SI Appendix*, Fig. S6). During this process, the heating up time showed negative relationship with the irradiation power and GO concentration, as shown in *SI Appendix*, Fig. S4, while the shrinkage capability of NIPAM was negatively correlated to GO and NIPAM concentration (*SI Appendix*, Fig. S5). Therefore, our surface demonstrated tunable wettability under NIR control for droplet manipulation.

To preliminary evaluate the droplet manipulation capacity of our constructed surface, the sliding of droplets under NIR irradiation was tested and monitored. Without NIR irradiation, the droplet was pinned to the surface because of the hydrophilic hydrogel arrays (*SI Appendix*, Fig. S7*A*). When irradiated by NIR light, the wettability arrays shrank back to interconnected holes to expose the porous and hydrophobic substrate, resulting in the sliding of water droplet (Fig. 3*A* and Movie S1). Based on the tunable wettability features of the surface, NIR masks were integrated with this system to supply programmable pathways for patterned control of droplets, as shown in *SI Appendix*, Fig. S7*B*. NIR masks only allowed part of the laser to arrive at the surface while blocking the other part of light. Thus the NIR-irradiated area would switch into hydrophobic status, yet the unexposed area remained hydrophilic, constructing a hydrophobic pathway for the sliding of droplets. Attractively, by designing different NIR masks, the surface could even produce several hydrophobic pathways for multiple droplets manipulation (Fig. 3 *B* and *C*). It is worth mentioning that the process is reversible under NIR irradiation and water immersion, demonstrating the repeatability and feasibility of the programmable surfaces. The water contact angles were measured for 10 cycles with NIR off/on to evidence the cyclic reproducibility (Fig. 3*D*). The results indicated the potential of our tunable and reversible wettability arrays for droplet manipulation technologies.

When the surfaces with wettability arrays were overturned, the droplets could well adhere to the substrate and be released by NIR control for droplet printing, as shown in Fig. 4*A*. To test this, droplets were dripped on a hydrophobic platform and then the platform was raised up to approach the test object. Because of the wettability arrays, the water droplets could be easily adhered to the surface. As irradiated by NIR, the GO-NIPAM hydrogel shrank back to the holes and then the water droplets were exposed to the hydrophobic substrate, resulting in their release (Fig. 4*B* and Movie S2). To investigate the contribution of GO-NIPAM to the wettability change, the surfaces with wettability arrays which are composed of different hydrogels were constructed and utilized for droplet-release test (*SI Appendix*, Fig. S8). The results indicated that GO-NIPAM hydrogel also facilitated the release of a droplet while other hydrogels could not. In addition to dealing with a single droplet, the GO-NIPAM–encapsulated substrate could also be used for manipulation of multiple droplets to meet high-throughput requirements. Here, a 4 × 4 array of droplets was constructed to test the manipulation capacity of our surface to multiple droplets (Fig. 4*C*). Similarly, the functional surface was employed to adhere the droplets array at the beginning. In this case, the droplets

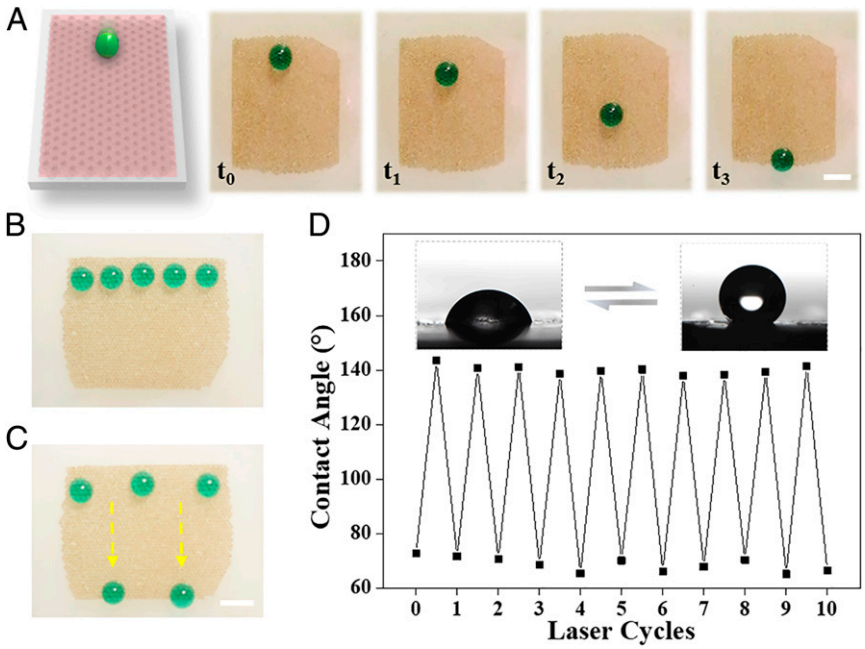

Fig. 3. (*A*) Sliding progress of a water droplet on the surface with wettability arrays under NIR irradiation. (*B* and *C*) Dynamic control of multiple droplets on the surface guided by designed pathways. (*D*) Water contact angle variation of the surface as a function of laser cycle numbers. (Scale bar: 0.25 cm.)

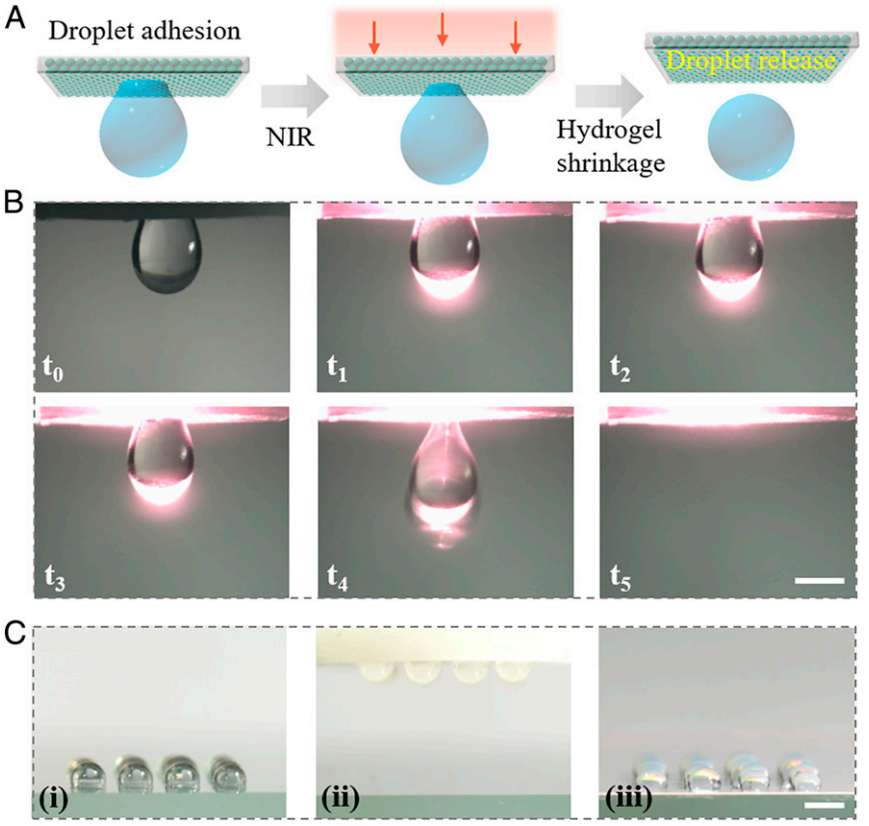

Fig. 4. (*A*) Schematic of the droplet release by surface with wettability arrays via NIR control. (*B*) Optical images of water droplet (10 μL) release from the surface. (*C*) Transfer of multiple droplets by the functional surface. (Scale bar: 2 mm in *B* and 0.25 cm in *C*.)

could be successfully transferred and then released on another substrate under remote control. These results demonstrated the potential of our tunable wettability surface in manipulation of droplets by switching hydrophilic and hydrophobic states for droplets printing.

To demonstrate the practical applications of the composite system with wettability arrays, the released droplets were utilized as microreactors for chemical reaction to synthesize nanoparticles and biomarker detection (Fig. 5*A*). As models for demonstration, $CdCl_2$ and Na_2S aqueous solution were chosen to synthesize CdS nanocrystals. When the droplet containing Na_2S was released to fuse with $CdCl_2$ droplet on the substrate, yellow materials immediately appeared at the interface, proving the successful synthesis of nanocrystals (Fig. 5*B*). After centrifugation, supernatant of the mixture droplet was characterized by a transmission electron microscope (TEM) which verified the existence of CdS nanocrystals. On this basis, the composite system was employed to manipulate multiple droplets for biological analysis. The probes were designed into hairpin structure to quench the fluorescence of carboxyfluorescein (FAM). Once the probes complementary bind with target molecules, the fluorescence signal would recover and the intensity would be positively related to the quantity of targets. Taking advantage of this principle, the probe droplets were released to react with different dilution of target droplets and demonstrated fluorescence signal with different intensity, as shown in Fig. 5*C*. This characteristic provides the possibility to realize the detection of multiple samples simultaneously with concentration gradients, greatly increasing the detection efficiency. These indicate the practical value of our bioinspired tunable wettability arrays in biomedical fields.

To further exploit the practical values of our surface with programmable wettability arrays, patterned photomasks were integrated in this system to control the radiation scope (Fig. 6*A*). Under this circumstance, only the illuminated area heated up and gave rise to the shrinkage of NIPAM hydrogel, thereby causing the selective release of multiple droplets into designed patterns, as shown in Fig. 6 *B* and *C*. Based on this characteristic, the wettability arrays could also be utilized in security field (Fig. 6*D*). Taking advantage of the controllable manipulation of multiple droplets, the composite system could encrypt the information which counts in various fields. As a concept demonstration, a two-dimensional (2D) code was designed to confirm the practical values of our system. Firstly, droplets with red fluorescence were released to the substrate with a 2D code pattern. Then the droplets with green and blue fluorescence were captured and released to the patterned location by the tunable wettability surface. In this case, the whole pattern presented vivid colors after the emission of UV, thus realizing the encryption of red fluorescence information. With the aid of a red filter, the hidden 2D code could be revealed from encryption status. It is worth mentioning that the droplets could realize more complicated and elaborate information encryption with appropriate design in a simple and versatile manner, demonstrating the potential value of our composite system with tunable wettability in various fields.

Discussion

In summary, we have presented a bioinspired hydrophobic surface with photocontrolled programmable wettability arrays by using microfluidics emulsification technique. Because of GO's photothermal property, the composite hydrogel arrays successfully switched the surface droplet adhesion status of system in

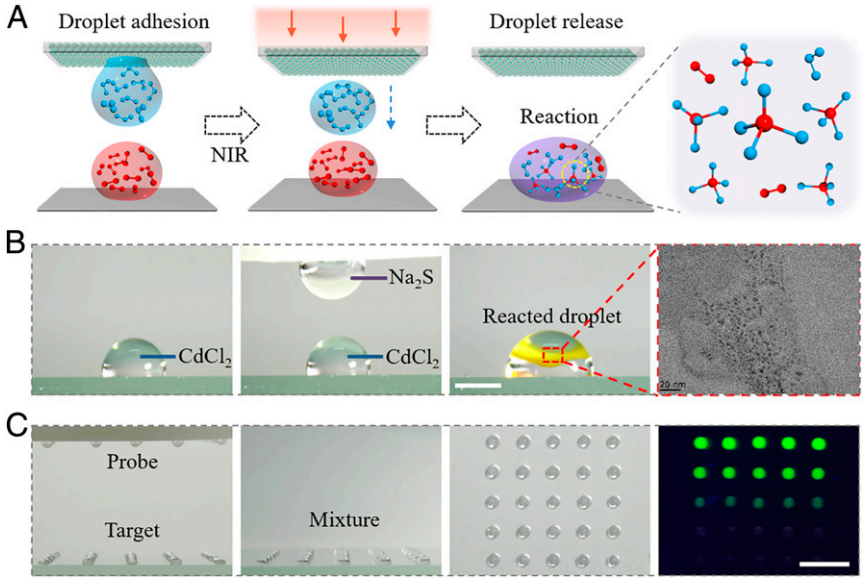

Fig. 5. (*A*) Schematic of the tunable wettability surface-assisted droplet-based microreactors. (*B*) Time-sequence images and TEM image showing the synthesis of CdS nanocrystals based on microreactors. (*C*) Optical images of the biological detection process using the droplet transfer capacity of tunable wettability surface. (Scale bar: 2 mm in *B* and 1 cm in *C*.)

response to remote NIR irradiation. Although many other techniques such as magnetic responsive fluid and geometry switch have been developed to construct tunable wettability surfaces, they have difficulty in satisfying accurate manipulation of droplets to a certain location or multiple locations. In comparison, by integrating NIR masks with different designs into our system, we have demonstrated controllable droplet sliding on programmable wettability pathways and effective droplet transfer

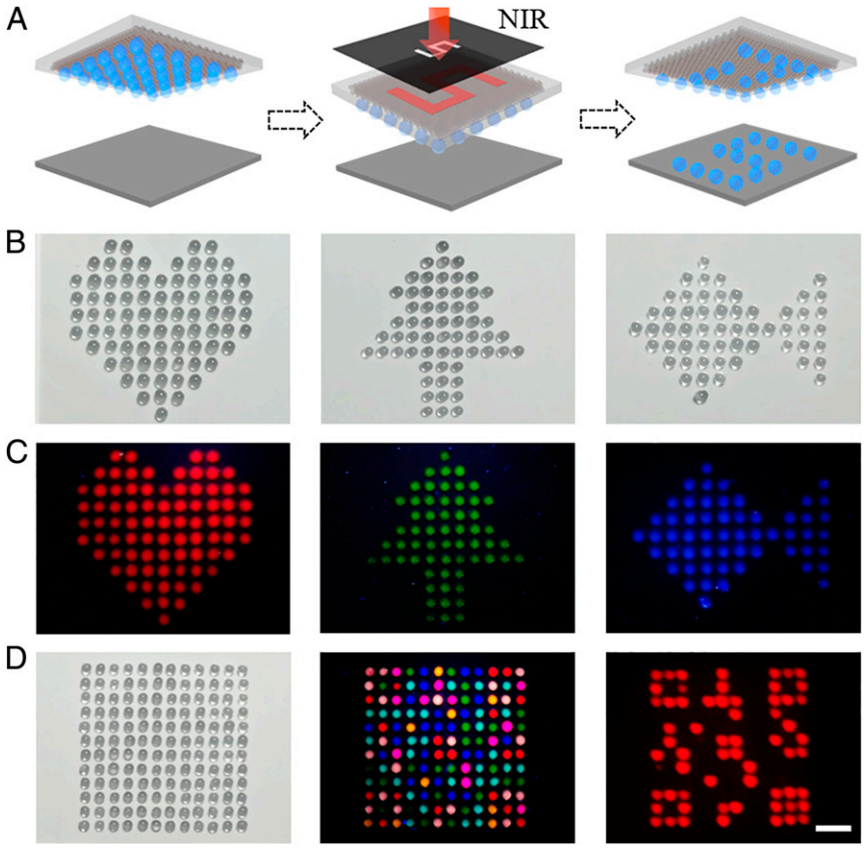

Fig. 6. (*A*) Schematic of patterned droplets' release from tunable wettability surface with integration of a photomask. (*B* and *C*) Optical images and corresponding fluorescence images of released droplets in different patterns. (*D*) A droplet array released from the surface with hidden 2D code information. (Scale bar: 1 cm.)

to provide microreactors for practical applications including biological detection, chemical synthesis, and printing. These features indicate that the surface with programmable wettability arrays have promising prospects in constructing intelligent droplet manipulation systems for multidisciplinary areas.

Materials and Methods

Materials. ETPTA resin (Mn = 428), NIPAM (97%), N, N′-methylenebis(acrylamide), photoinitiator 2-hydroxy-2-methylpropiophenone, and perfluorodecyl trimethoxysilane were bought from Sigma-Aldrich. Silica nanoparticles (SiO_2 nanoparticles, 250 nm) were obtained from DongJian Co. GO solution (10 mg/mL, XF NANO) was diluted to appropriate concentration for utilization. Dichloromethane was achieved from Sinopharm Chemical Reagent Co., Ltd. Ethanol was purchased from Sinopharm Chemical Reagent Co., Ltd. Deionized water was used in all experiments.

Microfluidics. The microfluidic device was coaxially assembled by two round and square capillaries on a glass slide. The inner glass capillary was tapered by a capillary puller (Sutter Instrument, P-97) to achieve the desired orifice that was measured by a microforge (MF-830). The diameter of the inner capillary orifice was 150–200 μm. The inner and outer diameters of collection capillary were 0.58 and 1 mm, respectively. Then the inner and collection capillaries were inserted into square capillary with inner diameter 1.0 5 mm. To seal the tubes, a transparent epoxy resin was employed where necessary. The dispersed phase was GO (2 mg/mL) hybrid NIPAM (10% wt/vol) and the continuous phase was SiO2 nanoparticles (10% wt/vol) dispersed ETPTA resin.

Fabrication of SiO_2 Nanoparticle-Dispersed ETPTA. SiO_2 nanoparticles were dispersed in ethanol firstly and then mixed with ETPTA resin under ultrasonication. After that, the mixture solution was placed in an oven (60 °C, 24 h) to remove ethanol and achieve ETPTA solution dispersed with SiO_2 nanoparticles. The resultant films were reserved in water for standby application.

Hydrophobic Treatment. The surfaces with hydrogel arrays were first treated by oxygen plasma to expose the abundant silicon hydroxyl on the ETPTA surface. Then the ETPTA membranes were placed together with dichloromethane solution containing 1% perfluorodecyl trimethoxysilane in an oven (60 °C) overnight. The hydrophobic surface with a perfluorodecyl trimethoxysilane layer deposition was obtained.

Characterization. The morphology features of the surfaces were observed by a field-emission scanning electron microscope (Ultra Plus, Zeiss) after freeze-drying treatment. The water contact angles (2 μL) were achieved by a JC2000D2 contact angle measuring system at room temperature (25 °C). The NIR irradiation system was bought from Xi Long Tech Co. Ltd. The temperature of the composite hydrogel was recorded by the uncooled handheld IR camera (FLIR Systems AB). Nanocrystals were characterized by a TEM (JEOL, JEM-2100). The video and optical images were recorded by an optical microscope (Olympus BX51) equipped with a charge-coupled device (CCD) camera (Media Cybernetics Evolution MP5.0) and a digital camera (Canon5D Mark II).

Data Availability. All data are contained in the manuscript text and *SI Appendix*.

ACKNOWLEDGMENTS. This work was supported by the National Natural Science Foundation of China (Grants 61927805 and 51522302), the National Natural Science Foundation of China (NSAF) (Grant U1530260), the Natural Science Foundation of Jiangsu (Grant BE2018707), the Scientific Research Foundation of Southeast University, and the Scientific Research Foundation of the Graduate School of Southeast University.

1. Z. Yang, J. Wei, Y. I. Sobolev, B. A. Grzybowski, Systems of mechanized and reactive droplets powered by multi-responsive surfactants. *Nature* **553**, 313–318 (2018).
2. X. Tang *et al*., Mechano-regulated surface for manipulating liquid droplets. *Nat. Commun.* **8**, 14831 (2017).
3. S. Zhang, J. Huang, Z. Chen, S. Yang, Y. Lai, Liquid mobility on superwettable surfaces for applications in energy and the environment. *J. Mater. Chem. A Mater. Energy Sustain.* **7**, 38–63 (2019).
4. C. Howell, A. Grinthal, S. Sunny, M. Aizenberg, J. Aizenberg, Designing liquid-infused surfaces for medical applications: A review. *Adv. Mater.* **30**, e1802724 (2018).
5. Y. Wu, J. Feng, H. Gao, X. Feng, L. Jiang, Superwettability-based interfacial chemical reactions. *Adv. Mater.* **31**, e1800718 (2019).
6. Y. Song *et al*., Budding-like division of all-aqueous emulsion droplets modulated by networks of protein nanofibrils. *Nat. Commun.* **9**, 2110 (2018).
7. Z. Huang *et al*., A general patterning approach by manipulating the evolution of two-dimensional liquid foams. *Nat. Commun.* **8**, 14110 (2017).
8. Q. Sun *et al*., Surface charge printing for programmed droplet transport. *Nat. Mater.* **18**, 936–941 (2019).
9. N. Li *et al*., Ballistic jumping drops on superhydrophobic surfaces via electrostatic manipulation. *Adv. Mater.* **30**, 1703838 (2018).
10. J. H. Jung, G. Destgeer, B. Ha, J. Park, H. J. Sung, On-demand droplet splitting using surface acoustic waves. *Lab Chip* **16**, 3235–3243 (2016).
11. L. Tian *et al*., Spontaneous assembly of chemically encoded two-dimensional coacervate droplet arrays by acoustic wave patterning. *Nat. Commun.* **7**, 13068 (2016).
12. G. Huang *et al*., Magnetically actuated droplet manipulation and its potential biomedical applications. *ACS Appl. Mater. Interfaces* **9**, 1155–1166 (2017).
13. S. Ben *et al*., Multifunctional magnetocontrollable superwettable-microcilia surface for directional droplet manipulation. *Adv. Sci. (Weinh.)* **6**, 1900834 (2019).
14. J. A. Lv *et al*., Photocontrol of fluid slugs in liquid crystal polymer microactuators. *Nature* **537**, 179–184 (2016).
15. L. Qi, Y. Niu, C. Ruck, Y. Zhao, Mechanical-activated digital microfluidics with gradient surface wettability. *Lab Chip* **19**, 223–232 (2019).
16. W. Wang *et al*., Multifunctional ferrofluid-infused surfaces with reconfigurable multiscale topography. *Nature* **559**, 77–82 (2018).
17. K. Liu, M. Vuckovac, M. Latikka, T. Huhtamäki, R. H. A. Ras, Improving surface-wetting characterization. *Science* **363**, 1147–1148 (2019).
18. T. Mouterde *et al*., Antifogging abilities of model nanotextures. *Nat. Mater.* **16**, 658–663 (2017).
19. J. Li *et al*, Topological liquid diode. *Sci. Adv.* **3**, eaao3530 (2017).
20. D. Chen, G. H. McKinley, R. E. Cohen, Spontaneous wettability patterning via creasing instability. *Proc. Natl. Acad. Sci. U.S.A.* **113**, 8087–8092 (2016).
21. M. Qin *et al*., Bioinspired hydrogel interferometer for adaptive coloration and chemical sensing. *Adv. Mater.* **30**, e1800468 (2018).
22. J. Wang *et al*., Bioinspired shape-memory graphene film with tunable wettability. *Sci. Adv.* **3**, e1700004 (2017).
23. D. Zhang *et al*., A smart superwetting surface with responsivity in both surface chemistry and microstructure. *Angew. Chem. Int. Ed. Engl.* **57**, 3701–3705 (2018).
24. B. Shang, M. Chen, L. Wu, NIR-triggered photothermal responsive coatings with remote and localized tunable underwater oil adhesion. *Small* **15**, e1901888 (2019).
25. H. Kim *et al*., Water harvesting from air with metal-organic frameworks powered by natural sunlight. *Science* **356**, 430–434 (2017).
26. J. Wang *et al*., Programmable wettability on photocontrolled graphene film. *Sci. Adv.* **4**, eaat7392 (2018).
27. H. Yin, A. L. Bulteau, Y. Feng, L. Billon, CO_2-induced tunable and reversible surface wettability of honeycomb structured porous films for cell adhesion. *Adv. Mater. Interfaces* **3**, 1500623 (2016).
28. X. Q. Dou, D. Zhang, C. Feng, L. Jiang, Bioinspired hierarchical surface structures with tunable wettability for regulating bacteria adhesion. *ACS Nano* **9**, 10664–10672 (2015).
29. H. Kim, S. J. Lee, Stomata-inspired membrane produced through photopolymerization patterning. *Adv. Funct. Mater.* **25**, 4496–4505 (2015).
30. A. Gargava, C. Arya, S. R. Raghavan, Smart hydrogel-based valves inspired by the stomata in plants. *ACS Appl. Mater. Interfaces* **8**, 18430–18438 (2016).
31. Y. Yu, L. Shang, J. Guo, J. Wang, Y. Zhao, Design of capillary microfluidics for spinning cell-laden microfibers. *Nat. Protoc.* **13**, 2557–2579 (2018).
32. T. Y. Lee *et al*., Microfluidic fabrication of capsule sensor platform with double-shell structure. *Adv. Funct. Mater.* **29**, 1902670 (2019).
33. H. Zhang, Y. X. Liu, J. Wang, C. M. Shao, Y. J. Zhao, Tofu-inspired microcarriers from droplet microfluidics for drug delivery. *Sci. China Chem.* **62**, 87–94 (2019).
34. Q. Pi *et al*., Digitally tunable microfluidic bioprinting of multilayered cannular tissues. *Adv. Mater.* **30**, e1706913 (2018).
35. Y. R. Yu, J. H. Guo, L. Y. Sun, X. X. Zhang, Y. J. Zhao, Bio-inspired micro-springs with ionic liquid encapsulation for flexible electronics. *Research* **2019**, 6906275 (2019).
36. P. Zhu, T. Kong, X. Tang, L. Wang, Well-defined porous membranes for robust omniphobic surfaces via microfluidic emulsion templating. *Nat. Commun.* **8**, 15823 (2017).
37. H. Wang *et al*, Biomimetic enzyme cascade reaction system in microfluidic electrospray microcapsules. *Sci. Adv.* **4**, eaat2816 (2018).
38. X. Yu *et al*., Graphene-based smart materials. *Nat. Rev. Mater.* **2**, 17046 (2017).
39. J. Wang *et al*., Responsive graphene oxide microcarriers for controllable cell capture and release. *Sci. China-Mater.* **61**, 1314–1324 (2018).